

## Thermal fluctuations of charged black holes in gravity's rainbow

Sudhaker Upadhyay<sup>a,b,\*</sup>, Seyed Hossein Hendi<sup>c,d,†</sup>, Shahram Panahiyan<sup>c,e,f,‡</sup> and Behzad Eslam Panah<sup>c,g,§</sup>

<sup>a</sup> *Department of Physics, K.L.S. College Nawada, Nawada-805110, Bihar, India*

<sup>b</sup> *Inter-University Centre for Astronomy and Astrophysics (IUCAA) Pune, Maharashtra-411007*

<sup>c</sup> *Physics Department and Biruni Observatory,*

*College of Sciences, Shiraz University, Shiraz 71454, Iran*

<sup>d</sup> *Research Institute for Astronomy and Astrophysics of Maragha (RIAAM), P.O. Box 55134-441, Maragha, Iran*

<sup>e</sup> *Helmholtz-Institut Jena, Fröbelstieg 3, Jena 07743, Germany*

<sup>f</sup> *Physics Department, Shahid Beheshti University, Tehran 19839, Iran and*

<sup>g</sup> *ICRANet, Piazza della Repubblica 10, I-65122 Pescara, Italy*

Quantum fluctuation effects have an irrefutable role in high energy physics. Such fluctuation can be often regarded as a correction of infrared (IR) limit. In this paper, the effects of the first-order correction of entropy, caused by thermal fluctuation, on the thermodynamics of charged black holes in gravity's rainbow will be discussed. It will be shown that such correction has profound contributions to high energy limit of thermodynamical quantities, stability conditions of the black holes and interestingly has no effect on thermodynamical phase transitions. The coupling between gravity's rainbow and the first-order correction will be addressed. In addition, the measurement of entropy as a function of fluctuation of temperature will be done and it will be shown that de Sitter (dS) case enforces an upper limit on the values of temperature and produces cyclic like diagrams. While for the anti-de Sitter (AdS) case, a lower limit on the entropy is provided and although for special cases a cyclic like behavior could be observed, no upper or lower limit exists for the temperature. In addition, a comparison between non-correction and correction included cases on the thermodynamical properties of solutions will also be discussed and the effects of the first-order correction will be highlighted. It will be shown that the first-order correction provides the solutions with larger classes of thermal stability conditions which may result into existence of a larger number of thermodynamical structures for the black holes.

### I. INTRODUCTION

Finding a consistent quantum theory of gravity is one of the interesting subjects in physics. Accordingly, a lot of attempts to join gravity and quantum theories together have been done. Nonetheless, there is no complete description of the quantum gravity yet. It is notable that, in order to construct a quantum theory of gravity, we have to investigate the validation of theory in the ultraviolet (UV) regime. On the other hand, it is arguable that Einstein's theory of general relativity is an effective theory which is valid in IR limit, while in UV regime it fails to produce accurate results. Therefore, this shortcoming requires modification in order to incorporate the UV regime. Horava-Lifshitz gravity is one of these theories which includes the UV regime by considering a modification of the usual energy-momentum relation [1, 2]. This theory reduces to general relativity (GR) in the IR limit. In other words, we can consider this theory as a UV completion of GR. Motivated by this work on Horava-Lifshitz gravity, different Lifshitz scaling for space and time have been considered for various theories, namely, type IIA string theory [3], type IIB string theory [4], dilatonic black branes [5, 6], dilatonic black holes [7, 8], and AdS/CFT correspondence [9–12].

It is notable that similar to the Horava-Lifshitz gravity, the gravity's rainbow (doubly GR) [13, 14], has also been viewed as a UV completion of GR. In doubly special relativity, there are two fundamental

---

\*Electronic address: sudhakerupadhyay@gmail.com; sudhaker@associates.iucaa.in

†Electronic address: hendi@shirazu.ac.ir

‡Electronic address: shahram.panahiyan@uni-jena.de

§Electronic address: behzad.eslampanah@gmail.com

constants; (i) the velocity of light, (ii) the Planck energy. In this theory, a particle cannot attain velocity and energy larger than the velocity of light and the Planck energy, respectively. Gravity's rainbow is a generalization of doubly special relativity to curved spacetime. In this theory of gravity, the energy of test particle affects the geometry of spacetime. In other words, gravity has different effects on the particles with various energies. So, the geometry of spacetime is represented by a family of energy-dependent metrics forming a rainbow of metrics. Similar to Horava-Lifshitz gravity, the gravity's rainbow can be constructed by considering a modification of the standard energy-momentum relation. The modification of usual energy-momentum relation in this gravity theory is given as

$$E^2 f^2(\varepsilon) - p^2 g^2(\varepsilon) = m^2, \quad (1)$$

with  $\varepsilon = E/E_p$ , where  $E$  and  $E_p$  are the energy of a test particle and the Planck energy, respectively. The functions  $f(\varepsilon)$  and  $g(\varepsilon)$  are called rainbow functions in which they are phenomenologically motivated and could be extracted by experimental data [15]. The rainbow functions are required to satisfy  $\lim_{\varepsilon \rightarrow 0} f(\varepsilon) = 1$  and  $\lim_{\varepsilon \rightarrow 0} g(\varepsilon) = 1$ , where these conditions ensure that modified energy-momentum relation reduces to the usual one in the IR limit. It is worthwhile to mention that the energy of a test particle ( $E$ ) cannot be greater than  $E_p$ . It means that if a test particle is used to probe the geometry of spacetime, then  $E$  is always smaller than  $E_p$  (see Ref. [16], for more details). It is notable that such justification is based on the Standard model of particle physics. Also, considering a suitable choice of the rainbow functions, the Horava-Lifshitz gravity can be related to the gravity's rainbow [17]. It should be noted that since it was shown that specific models of gravity's rainbow could be related to Horava-Lifshitz gravity [17], one can argue that, by suitable transformations, the thermal effects obtained and investigated here, could be mapped to Horava-Lifshitz results with specific scaling parameter. This enables one to perform study in less complex framework and map it later to a more sophisticated one (similar to the AdS/CFT correspondence approach).

One of the most important results of the UV completion of geometries is modification at the last stage of evaporation of black holes. In the IR limit where gravity's rainbow yields general relativity, the thermodynamics of black holes in gravity's rainbow reduces to the usual one which is observed for large black holes. On the contrary, in case of the black holes evaporation and reduction in their size, the black hole thermodynamics in gravity's rainbow shows significant deviation from the usual black hole thermodynamics. Especially, such deviation becomes more evident at the end stage of evaporation of black hole in gravity's rainbow [18]. At this stage, the temperature of black holes acquires a maximum value, and then it decreases beyond this maximum value. At a critical point, while size of the black hole is non-zero, its temperature vanishes and, therefore, there is no Hawking radiation. This indicates the existence of a black hole remnant in gravity's rainbow. Formation and existence of a black hole remnant play a crucial role in phenomenological consequences for the detection of mini black holes at the LHC [18]. In order to incorporate the upper bound on the energy of a particle, the usual uncertainty principle has to be modified to a generalized one. The particle probes the geometry of black hole and it also fixes the energy scale of the gravity's rainbow. This provides the possibility of using the bound on the energy of a particle emitted in the Hawking radiation as an energy scale in the rainbow functions.

Black hole solutions and their thermodynamical properties have been obtained in gravity's rainbow, and it was shown that the rainbow functions modify the thermodynamical properties of obtained black holes in this theory [18–27]. Also effects of gravity's rainbow on the thermodynamical properties and phase transition of black holes have been investigated in Gauss-Bonnet [28], Kaluza-Klein [29], massive [30, 31], F(R) [32, 33], and dilaton [34, 35] gravities. Electric charge and magnetic monopoles in gravity's rainbow have been studied in Ref. [36]. In the context of gravity's rainbow, the possibility of quantum fluctuations to induce a topological change has been studied [37]. Using the gravity's rainbow, the hydrostatic equilibrium for compact objects and the structure of neutron stars have also been investigated in Refs. [38, 39]. The effects of rainbow function on wormholes have been studied in Ref. [41]. Cosmic string and black rings in gravity's rainbow have been obtained in Refs. [42] and [43], respectively. Metric structures of this theory such as; the original rainbow metrics proposal, the momentum-space-inspired metric and the standard Finsler geometry approach have been perused in Ref. [44]. The effects of rainbow functions on the geodesics around the black holes have been studied in Ref.[45]. Another interesting result of this gravity is related to the FRW cosmology in which it was shown that employing this formalism

will provide the possibility of removing the big bang singularity [46–49], and the big bounce of a cyclic universe [50]. For more investigations regarding the gravity’s rainbow, see Refs. [51–61].

Moreover, it has been observed that thermodynamics of black hole undergoes corrections due to the thermal fluctuations. The various approaches, namely, field theory methods [62, 63], quantum geometry techniques [64, 65], general statistical mechanical arguments [66] and Cardy formula [67] had confirmed that leading-order corrections to the entropy originated due to the thermal fluctuations are logarithmic in nature. The consequences of these corrections on the various black hole thermodynamics have been studied with great interests [68–71]. For instance, recently, the role of thermal fluctuations has been studied in the contexts of Schwarzschild-Beltrami-de Sitter black hole [72] and the massive black hole in AdS space [73]. Similar analysis has also been made on the modified Hayward black hole, where it is found that thermal fluctuation plays an important role in order to reduce pressure and internal energy of the Hayward black hole [74]. The importance of logarithmic correction to the area law can also be seen in the study of quark-gluon plasma properties through holographic principles [75, 76]. Our motivation, here, is to study the effects of thermal fluctuations on the thermodynamics of charged black hole in gravity’s rainbow.

The paper is presented as follows. In Sec. II, we discuss the charged black hole in gravity’s rainbow. We study the effects of thermal fluctuation on various thermodynamical quantities in Sec. III. The effects of the first-order correction on thermal stability are discussed in Sec. IV. Section V devoted to investigate the correction case versus the non-correction one on thermodynamical properties of the solutions. We, finally, conclude our results in the last section.

## II. CHARGED BLACK HOLES IN GRAVITY’S RAINBOW

The Lagrangian density of Einstein gravity with cosmological constant coupled to an electromagnetic field is given by

$$L = R - 2\Lambda - L_{Max}, \quad (2)$$

where  $L_{Max} = F_{ab}F^{ab}$  is the Maxwell’s Lagrangian.

The equations of motion corresponding to the metric tensor  $g_{ab}$  and the Faraday tensor  $F_{ab}$  are respectively

$$R_{ab} + g_{ab} \left( \Lambda(\varepsilon) - \frac{1}{2}R \right) + 2 \left( F_{ac}F_b^c - \frac{1}{4}g_{ab}F_{cd}F^{cd} \right) = 0, \quad (3)$$

$$\partial_a(\sqrt{-g}F^{ab}) = 0, \quad (4)$$

where  $\Lambda(\varepsilon)$  is the energy-dependent cosmological constant. The energy-dependent metric for gravity’s rainbow is defined by

$$ds^2 = -\frac{\psi(r, \varepsilon)}{f^2(\varepsilon)} + \frac{dr^2}{g^2(\varepsilon)\psi(r, \varepsilon)} + \frac{r^2}{g^2(\varepsilon)}h_{ij}dx^i dx^j, \quad i, j = 1, 2. \quad (5)$$

where  $h_{ij}dx^i dx^j$  is the spacial line element with constant curvature  $2k$ . The incorporation of gauge potential ansatz  $A_a = h(r, \varepsilon)\delta_a^0$  in the Maxwell equation (4) yields

$$h(r, \varepsilon) = -\frac{q(\varepsilon)}{r}, \quad (6)$$

where  $q(\varepsilon)$  is as integration constant related to the electrical charge. Here, the electric charge is an invariant quantity. We know that  $q(\varepsilon)$  is an integration constant which is proportional to electric charge. It is notable that the integration constant can be energy dependent, too. In order to clarify this point, we can regard  $q(\varepsilon) = g(\varepsilon)^a f(\varepsilon)^b q$  with arbitrary  $a$  and  $b$  and  $q$  is the invariant electric charge. Also, it leads

to the following nonzero component of electromagnetic field tensor  $F_{rt} = \frac{q(\varepsilon)}{r^2}$ . The equation of motion (3) leads to

$$\psi'(r, \varepsilon)g^2(\varepsilon)r + (\psi(r, \varepsilon) - k)g^2(\varepsilon) + \Lambda(\varepsilon)r^2 + \frac{q^2(\varepsilon)g^2(\varepsilon)f^2(\varepsilon)}{r^2} = 0, \quad (7)$$

which has the following solution:

$$\psi(r, \varepsilon) = k - \frac{m_0(\varepsilon)}{r} - \frac{\Lambda(\varepsilon)r^2}{3g^2(\varepsilon)} + \frac{q^2(\varepsilon)f^2(\varepsilon)}{r^2}, \quad (8)$$

where  $m_0(\varepsilon)$  is an integration constant related to the total mass of the black hole. We note that, in the GR limit (i.e.,  $f(\varepsilon) \rightarrow 1$  and  $g(\varepsilon) \rightarrow 1$ ), the solution (8) reduces to the Reissner-Nordström black hole in 4-dimensions. Here, one may take  $k = 1, 0, -1$ , corresponding to a spherical, Ricci flat, hyperbolic horizon for the black hole, respectively.

### III. THERMODYNAMICAL QUANTITIES

It is possible to obtain the Hawking temperature by using the surface gravity as follows,

$$\begin{aligned} T_H &= \frac{g(\varepsilon)}{4\pi f(\varepsilon)} \psi'(r, \varepsilon)|_{r=r_+}, \\ &= \frac{1}{4\pi} \left( \frac{kg(\varepsilon)}{f(\varepsilon)r_+} - \frac{\Lambda(\varepsilon)r_+}{g(\varepsilon)f(\varepsilon)} - \frac{q^2(\varepsilon)g(\varepsilon)f(\varepsilon)}{r_+^3} \right), \end{aligned} \quad (9)$$

in which  $r_+$  is related to the event horizon of black hole. it can be seen here that in the GR limit (i.e.,  $f(\varepsilon) \rightarrow 1$  and  $g(\varepsilon) \rightarrow 1$ ), we recover the Hawking temperature of charged black holes. As we know that the thermal fluctuations correct thermodynamical quantities. To the leading order, the entropy gets logarithmic correction [66, 77] and given by,

$$S = S_0 - \frac{\alpha}{2} \log(S_0 T_H^2), \quad (10)$$

where  $\alpha$  is a dimensional full parameter and the zeroth-order entropy in four-dimensions is given by [24]

$$S_0 = \frac{\pi r_+^2}{4g^2(\varepsilon)}. \quad (11)$$

Exploiting relations (9), (10) and (11), we get explicit expression of first-order corrected entropy as

$$S = \frac{\pi r_+^2}{4g^2(\varepsilon)} - \alpha \log \left[ \frac{1}{8\sqrt{\pi}} \left( \frac{k}{f(\varepsilon)} - \frac{\Lambda(\varepsilon)r_+^2}{g^2(\varepsilon)f(\varepsilon)} - \frac{q^2(\varepsilon)f(\varepsilon)}{r_+^2} \right) \right]. \quad (12)$$

Utilizing the definitions of entropy and temperature, we are able to compute the Helmholtz function with following relation:  $F = -\int SdT_H$ . Here, the Helmholtz function is calculated by

$$\begin{aligned} F &= \frac{1}{16} \left( \frac{kr_+}{f(\varepsilon)g(\varepsilon)} + \frac{1}{3} \frac{\Lambda(\varepsilon)r_+^3}{g^3(\varepsilon)f(\varepsilon)} + \frac{3q^2(\varepsilon)f(\varepsilon)}{g(\varepsilon)r_+} \right) + \frac{\alpha}{6\pi} \frac{q^2(\varepsilon)f(\varepsilon)g(\varepsilon)}{r_+^3} \\ &+ \frac{\alpha}{2\pi} \frac{\Lambda(\varepsilon)r_+}{f(\varepsilon)g(\varepsilon)} - \frac{\alpha}{4\pi} \left( \frac{q^2(\varepsilon)f(\varepsilon)g(\varepsilon)}{r_+^3} - \frac{kg(\varepsilon)}{f(\varepsilon)r_+} + \frac{\Lambda(\varepsilon)r_+}{f(\varepsilon)g(\varepsilon)} \right) \log \left[ \frac{1}{8\sqrt{\pi}} \left( \frac{k}{f(\varepsilon)} \right. \right. \\ &\left. \left. - \frac{\Lambda(\varepsilon)r_+^2}{g^2(\varepsilon)f(\varepsilon)} - \frac{q^2(\varepsilon)f(\varepsilon)}{r_+^2} \right) \right]. \end{aligned} \quad (13)$$

Using the Hamiltonian approach, one can find the uncorrected mass  $M$  of the black hole for gravity's rainbow as [30]

$$M = \frac{m_0}{8f(\varepsilon)g(\varepsilon)}, \quad (14)$$

where  $m_0$  is evaluated by setting metric function to zero on horizon ( $\psi(r, \varepsilon)|_{r=r_+} = 0$ ) as

$$m_0 = kr_+ - \frac{\Lambda(\varepsilon)r_+^3}{3g^2(\varepsilon)} + \frac{q^2(\varepsilon)f^2(\varepsilon)}{r_+}. \quad (15)$$

Here we note that the mass calculated here is not a corrected mass. In other words, using this mass with first law of black hole thermodynamics does not yield desirable result. To solve this problem, we use thermodynamical approach in calculating mass. In order to calculate the corrected mass  $M$ , we employ the concepts of thermodynamics and use the following thermodynamical relation:

$$\begin{aligned} M &= F + T_H S, \\ &= \frac{1}{8} \left( \frac{kr_+}{f(\varepsilon)g(\varepsilon)} - \frac{1}{3} \frac{\Lambda(\varepsilon)r_+^3}{g^3(\varepsilon)f(\varepsilon)} + \frac{q^2(\varepsilon)f(\varepsilon)}{g(\varepsilon)r_+} \right) + \frac{\alpha}{6\pi} \frac{q^2(\varepsilon)f(\varepsilon)g(\varepsilon)}{r_+^3} \\ &\quad + \frac{\alpha}{2\pi} \frac{\Lambda(\varepsilon)r_+}{f(\varepsilon)g(\varepsilon)}. \end{aligned} \quad (16)$$

Obtained mass here could be used alongside of first law of black hole thermodynamics to ensure the validity of calculated thermodynamical quantities. The electric charge is calculated from the flux of the electric field at infinity as follows,

$$Q = \frac{q(\varepsilon)f(\varepsilon)}{4g(\varepsilon)}. \quad (17)$$

The electric (chemical) potential  $U$ , can be defined as the gauge potential at the event horizon with respect to the reference

$$U = A_\mu \chi^\mu |_{r \rightarrow \infty} - A_\mu \chi^\mu |_{r \rightarrow r_+} = \frac{q(\varepsilon)}{r_+}. \quad (18)$$

The first-order corrected Gibbs free energy for this black holes is given by

$$\begin{aligned} G &= F - UQ, \\ &= \frac{1}{16} \left( \frac{k}{f(\varepsilon)g(\varepsilon)} r_+ + \frac{1}{3} \frac{\Lambda(\varepsilon)r_+^3}{g^3(\varepsilon)f(\varepsilon)} - \frac{q^2(\varepsilon)f(\varepsilon)}{g(\varepsilon)r_+} \right) + \frac{\alpha}{6\pi} \frac{q^2(\varepsilon)f(\varepsilon)g(\varepsilon)}{r_+^3} \\ &\quad + \frac{\alpha}{2\pi} \frac{\Lambda(\varepsilon)r_+}{f(\varepsilon)g(\varepsilon)} - \frac{\alpha}{4\pi} \left( \frac{q^2(\varepsilon)f(\varepsilon)g(\varepsilon)}{r_+^3} - \frac{kg(\varepsilon)}{f(\varepsilon)r_+} + \frac{\Lambda(\varepsilon)r_+}{f(\varepsilon)g(\varepsilon)} \right) \log \left[ \frac{1}{8\sqrt{\pi}} \left( \frac{k}{f(\varepsilon)} \right. \right. \\ &\quad \left. \left. - \frac{\Lambda(\varepsilon)r_+^2}{g^2(\varepsilon)f(\varepsilon)} - \frac{q^2(\varepsilon)f(\varepsilon)}{r_+^2} \right) \right]. \end{aligned} \quad (19)$$

Now, it is easy to establish the first law of black hole by using thermodynamical quantities such as temperature (9), entropy (12), charge (17), electric potential (18) and corrected mass (16),

$$dM = T_H dS + U dQ.$$

Our next quantity of interest is heat capacity. The importance of this quantity lies in the fact that condition for thermal stability and phase transition points could be extracted using this quantity. The

heat capacity of these black holes could be calculated as

$$\begin{aligned}
C &= \frac{T_H}{\left(\frac{\partial^2 M}{\partial S^2}\right)_Q} = \frac{T_H}{\left(\frac{\partial T_H}{\partial S}\right)_Q} = \frac{\partial M}{\partial T_H}, \\
&= -\frac{\pi r_+^2}{2g(\varepsilon)} \left( \frac{kg^2(\varepsilon)r_+^2 - \Lambda(\varepsilon)r_+^4 - q^2(\varepsilon)g^2(\varepsilon)f^2(\varepsilon)}{kg^2(\varepsilon)r_+^2 + \Lambda(\varepsilon)r_+^4 - 3q^2(\varepsilon)g^2(\varepsilon)f^2(\varepsilon)} \right) \\
&+ 2\alpha \left( \frac{q^2(\varepsilon)f^2(\varepsilon)g^2(\varepsilon) - \Lambda(\varepsilon)r_+^4}{kg^2(\varepsilon)r_+^2 + \Lambda(\varepsilon)r_+^4 - 3q^2(\varepsilon)g^2(\varepsilon)f^2(\varepsilon)} \right). \tag{20}
\end{aligned}$$

In next section, we will investigate the thermodynamical behavior of the solutions and highlight the effects of entropy correction in details.

#### IV. THERMAL STABILITY

Our main motivation here is to understand how the first-order correction would modify thermodynamical behavior of the solutions. First, we start with mass. It was seen that uncorrected version of the mass (14) does not yield suitable results considering the concept of the first law of black hole thermodynamics. Therefore, we calculated the corrected version using thermodynamical concept (16).

Evidently, the corrected mass is modified due to presence of the first-order correction. The mass here is an increasing function of the correction parameter,  $\alpha$ . In addition, due to presence of the correction, two new terms are added to mass. These two terms  $\left(\frac{\alpha}{6\pi} \frac{q^2(\varepsilon)f(\varepsilon)g(\varepsilon)}{r_+^3}\right)$  and  $\frac{\alpha}{2\pi} \frac{\Lambda(\varepsilon)r_+}{f(\varepsilon)g(\varepsilon)}$  of (16)) include electric charge coming from the matter field contribution and cosmological constant which could be understood as a generalization of the gravitational sector. Interestingly, there is no coupling between the topological factor,  $k$ , and correction parameter,  $\alpha$ . This signals the fact that first-order correction affects the gravitational and matter field sectors while it does not have any effect on topological structure. In addition, the thermodynamical behavior of the mass, hence internal energy, in high energy regime (very small  $r_+$ ) is governed by the term in which electric charge and correction parameter are coupled (term  $\frac{\alpha}{6\pi} \frac{q^2(\varepsilon)f(\varepsilon)g(\varepsilon)}{r_+^3}$  in Eq. (16)). This indicates that for high energy limit, the contribution of the first-order correction is dominant and highlighted. On the other hand, the asymptotical behavior of the mass is governed by  $\Lambda$  term without correction which shows the absence of effects of the first-order correction for this limit (term  $\frac{-1}{24} \frac{\Lambda(\varepsilon)r_+^3}{g^3(\varepsilon)f(\varepsilon)}$  in Eq. (16)). Interestingly, the topological term and correction term coupled with cosmological constant have same order of horizon radius. By suitable choices of different parameter ( $k = -\frac{4\alpha}{\pi}\Lambda(E)$ ), it is possible to omit the effects of topological term. This indicates that by this choice, one can eliminate the effects of topological structure on thermodynamical behavior of the mass. In other words, total behavior of the mass would be independent of the geometrical structure of horizon (hence, topological factor). On the other hand, due to this property, one can state that medium class of the black holes are also affected by the existence of first-order correction. To summarize, one can state that small and medium black holes are affected by the presence of first-order correction while large black holes are not affected on significant level.

In classical thermodynamics of the black holes, negativity of the internal energy, hence mass signals the absence of physical black holes. It is a matter of calculation to obtain the root for mass of this black hole in the following form:

$$r_+(M=0) = \sqrt{\frac{g(\varepsilon)}{2\pi\Lambda(\varepsilon)} \left[ \mathcal{A}^{1/3} + \frac{4\mathcal{B}}{\mathcal{C}^{1/3}} + 2g(\varepsilon)(\pi k + 4\alpha\Lambda(\varepsilon)) \right]}, \tag{21}$$

in which  $\mathcal{A}$ ,  $\mathcal{B}$  and  $\mathcal{C}$  have following forms:

$$\mathcal{A} = 96\alpha g(\varepsilon)\Lambda(\varepsilon)\left\{g^2(\varepsilon)\left[\frac{16}{3}\alpha^2\Lambda^2(\varepsilon) + 4\pi k\alpha\Lambda(\varepsilon) + \pi^2k^2\right] + \frac{2\pi}{3}q^2(\varepsilon)f^2(\varepsilon)\Lambda(\varepsilon)\right\} \\ + 4\pi^3kg(\varepsilon)\left[3q^2(\varepsilon)f^2(\varepsilon)\Lambda(\varepsilon) + 2k^2g^2(\varepsilon)\right] + \mathcal{G},$$

$$\mathcal{B} = g^2(\varepsilon)\left[\pi k + 4\alpha\Lambda(\varepsilon)\right]^2 + \pi^2q^2(\varepsilon)f^2(\varepsilon)\Lambda(\varepsilon),$$

$$\mathcal{C} = 8g(\varepsilon)\left\{g^2(\varepsilon)\left[\pi k + 4\alpha\Lambda(\varepsilon)\right]^3 + \frac{3\pi^2}{2}q^2(\varepsilon)f^2(\varepsilon)\Lambda(\varepsilon)\left[\pi k + \frac{16}{3}\alpha\Lambda(\varepsilon)\right]\right\} + \mathcal{G},$$

with

$$\mathcal{G} = 4\pi q(\varepsilon)f(\varepsilon)\Lambda(\varepsilon)\left[16\alpha g^4(\varepsilon)\left[\pi k + 4\alpha\Lambda(\varepsilon)\right]^3 \right. \\ \left. - 3\pi^2q^2(\varepsilon)g^2(\varepsilon)f^2(\varepsilon)\left[\pi^2k^2 - \frac{64}{3}\alpha^2\Lambda^2(\varepsilon)\right] - 4\pi^4q^4(\varepsilon)f^4(\varepsilon)\Lambda(\varepsilon)\right]^{1/2}.$$

Studying the root shows that the physical region for the existence of the black hole is a function of the correction. In other words, depending on choices of this parameter, the physical region for the existence of black holes would be modified. In order to understand the details regarding the behavior of the mass, we have plotted two sets of diagrams for cases of dS (left panel of Fig. 1) and AdS black holes (right panel of Fig. 1). Evidently, for AdS case, mass enjoys a minimum in its structure and it does not acquire root. On the other hand, dS case enjoys one minimum, one maximum and one root in its structure. The root is located after the extrema. After root, the mass is negative which indicates that existence of black holes in dS picture is limited to a specific region while for the AdS case, such limit does not exist. The place of the root is an increasing function of the correction parameter. This means that comparing to uncorrected version, in the presence of first-order correction, the region of positivity of mass, hence internal energy, is bigger which indicates that physical black holes with larger horizon are obtainable in the presence of this correction.

Next, we turn our attention to temperature. The temperature is independent of the first-order correction. This means that although that entropy and mass of the black holes are affected by the presence of first-order correction, the temperature is free of it. This shows that presence of the first-order correction modified the thermodynamical structure of these black holes on a specific level and introduced the following property: the entropy is a decreasing function of the correction parameter. This means that by increasing this parameter, the disorder which is represented by entropy, increases. Therefore, one expects to see the modification in temperature. But, the correction also affects the internal energy on a certain level. This modification combined with one in entropy provides a framework in which increasing the disorder in the system will be defined by the modification in internal energy on a level which results into the absence of modification in temperature. Specifically speaking, modification in entropy which is caused due to the presence of the first-order correction is controlled by changes in internal energy which leads to the temperature being independent of this parameter. This is somehow similar to the isothermal process in which the temperature remains the same. This is one of the most important properties of black holes with the first-order correction. They present isothermal-like behavior for modifications in correction parameter.

The high energy limit of temperature is governed by the term with electric charge while for the asymptotical behavior the cosmological term plays the key role (see Eq. (9)). It is a matter of calculation to obtain the roots of the temperature in the following manner:

$$r_+(T=0) = \pm \frac{\sqrt{2g(\varepsilon)\Lambda(\varepsilon)\left[kg(\varepsilon) + \sqrt{k^2g^2(\varepsilon) \pm 4q^2(\varepsilon)f^2(\varepsilon)\Lambda(\varepsilon)}\right]}}{2\Lambda(\varepsilon)}. \quad (22)$$

Evidently, the existence of root of the solutions depends on satisfaction of the following conditions:

$$k^2 \geq \frac{4q^2(\varepsilon) f^2(\varepsilon) \Lambda(\varepsilon)}{g^2(\varepsilon)}, \quad \& \quad \Lambda(\varepsilon) \left[ kg(\varepsilon) \pm \sqrt{k^2 g^2(\varepsilon) - 4q^2(\varepsilon) f^2(\varepsilon) \Lambda(\varepsilon)} \right] \geq 0.$$

Here too, similar to the mass case, we employed numerical evaluation to understand the behavior of the temperature in more details (see Fig. 2). For dS case, depending on choices of different parameters, the temperature could enjoy one of the following cases: I) two roots with one maximum are located between them, II) One maximum which is also the root of temperature and III) one maximum without any root. In the first case, the physical solutions (positive temperature) exists only between the roots, whereas for the other two cases, the temperature is negative for any horizon radius, therefore no physical black hole exists. As for AdS case, temperature could have one of the following cases: I) only one root and temperature is an increasing function of horizon radius, II) one root with one extremum (extremum is located after root) and III) one root, one maximum and one minimum. Presence of extremum in temperature signals the existence of phase transition point for the black holes. In other words, extrema of the temperature are those points where the system goes through phase transitions. Considering the behavior of the temperature in dS and AdS cases, one can conclude that dS black holes enjoy the existence of physical phase transition only in one case (the case with two roots) whereas AdS ones, depending on choices of different parameters, could have one or no phase transition. Considering that thermal phase transition takes place between thermally unstable black holes and stable ones, we need to study the heat capacity to see what type of phase transitions are present in the structure of these black holes for dS and AdS cases.

The heat capacity, contrary to temperature is correction dependent. Interestingly, the presence of correction parameter,  $\alpha$ , is only observed in the numerator of heat capacity (20). This indicates that the first-order correction only affects the places of root while the phase transition points (divergencies of the heat capacity) are independent of this parameter. It is a matter of calculation to obtain roots and divergences of the heat capacity in the following form:

$$r_+(C=0) = \frac{1}{2^{4/3}} \sqrt{\frac{g(\varepsilon)}{6\pi\Lambda(\varepsilon)}} \left( \frac{\mathcal{Y}}{\mathcal{P}} \right), \quad (23)$$

$$r_+(C \rightarrow \infty) = \pm \frac{\sqrt{-2\Lambda(\varepsilon)g(\varepsilon) \left[ kg(\varepsilon) \pm \sqrt{k^2 g^2(\varepsilon) + 12q^2(\varepsilon) f^2(\varepsilon) \Lambda(\varepsilon)} \right]}}{2\Lambda(\varepsilon)}, \quad (24)$$

in which

$$\begin{aligned} \mathcal{Y} &= 2^{4/3} \mathcal{Z}^{2/3} + 2^{5/3} \pi k g(\varepsilon) \mathcal{Z}^{1/3} + 2^{14/3} g(\varepsilon) \sqrt{\alpha \Lambda(\varepsilon)} \mathcal{Z}^{1/3} \\ &+ 4g^2(\varepsilon) [\pi k + 4\alpha \Lambda(\varepsilon)]^2 - 12\pi^2 q^2(\varepsilon) f^2(\varepsilon) \Lambda(\varepsilon), \end{aligned}$$

$$\mathcal{P} = \sqrt{\pi \Lambda(\varepsilon)} \mathcal{Z}^{1/6},$$

$$\begin{aligned} \mathcal{Z} &= 2g(\varepsilon) \left[ g^2(\varepsilon) (\pi k + 4\alpha \Lambda(\varepsilon))^3 - \frac{9\pi^2}{2} q^2(\varepsilon) f^2(\varepsilon) \Lambda(\varepsilon) [\pi k + 16\alpha \Lambda(\varepsilon)] \right] \\ &+ 3q(\varepsilon) f(\varepsilon) \Lambda(\varepsilon) \mathcal{H}, \end{aligned}$$

with

$$\begin{aligned} \mathcal{H} &= \left[ -48\alpha g^4(\varepsilon) [\pi k + 4\alpha \Lambda(\varepsilon)]^3 - 3\pi^2 q^2(\varepsilon) g^2(\varepsilon) f^2(\varepsilon) [\pi^2 k^2 \right. \\ &\left. - 704\alpha^2 \Lambda^2(\varepsilon) - 64\pi \alpha k \Lambda(\varepsilon)] + 12\pi^4 q^4(\varepsilon) f^4(\varepsilon) \Lambda(\varepsilon) \right]. \end{aligned}$$



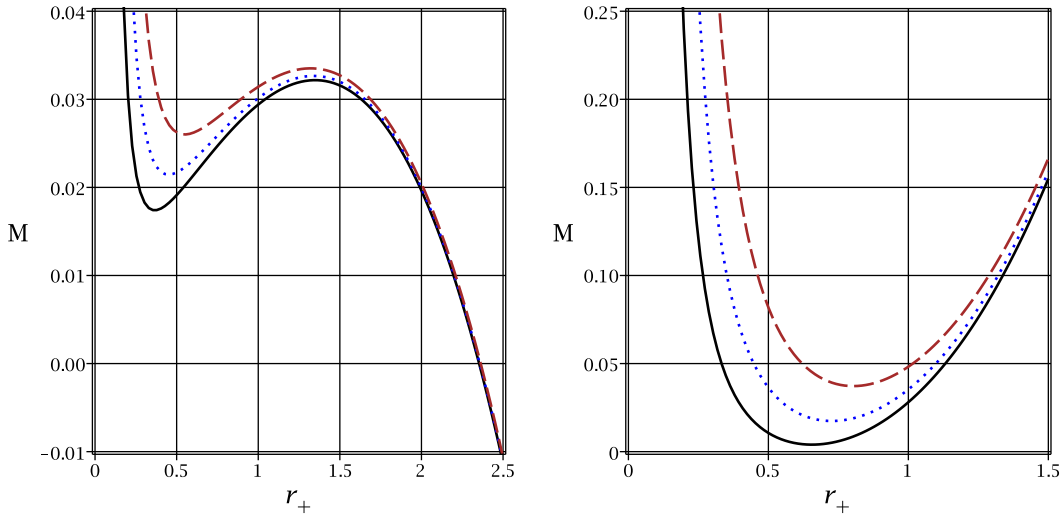


FIG. 1:  $M$  versus  $r_+$  for  $f(\varepsilon) = g(\varepsilon) = 0.9$ ,  $k = \alpha = 1$ ,  $q(\varepsilon) = 0.2$  (continuous line),  $q(\varepsilon) = 0.2887$  (dotted line) and  $q(\varepsilon) = 0.4$  (dashed line). Left panel:  $\Lambda(\varepsilon) = 1$ ; Right panel:  $\Lambda(\varepsilon) = -1$ .

Existence of the divergence point for the solutions is limited to satisfaction of the following conditions

$$k^2 \geq -\frac{12\Lambda(\varepsilon)q^2(\varepsilon)f^2(\varepsilon)}{g^2(\varepsilon)}, \quad \& \quad \Lambda(\varepsilon) \left[ -kg(\varepsilon) \pm \sqrt{k^2g^2(\varepsilon) + 12\Lambda(\varepsilon)q^2(\varepsilon)f^2(\varepsilon)} \right] \geq 0.$$

The first condition is always satisfied for dS black holes. Considering that square root function is always positive valued and by taking the structure of conditions into account, one can conclude that there is always a divergence point for the dS black holes. In addition, the dS case enjoys the existence of two roots in its heat capacity. As for the AdS black holes, the situation is more complicated. Depending on choices of different parameters, these black holes could enjoy one of the following cases: I) two divergence points with one root located between them, II) one divergence point and one root in which root is observed after divergence point, and III) only one root is observable. In order to elaborate these results, we have plotted the diagrams (see Fig. 2).

In order to make accurate predictions regarding thermodynamical properties of these black holes, one must consider the thermodynamical behavior of temperature alongside with the heat capacity. The reason is that negativity/positivity of the temperature enforces a harder restriction on values that different parameters can acquire. This is due to fact that negative values of the temperature are considered as non-physical cases. For the dS case, the heat capacity enjoys the existence of one divergence and two roots. The roots are located after the divergence. Between the root of the temperature and divergence of the heat capacity, the heat capacity is negative valued and solutions are thermally unstable. At the divergence of heat capacity, a phase transition between smaller unstable and larger stable black holes takes place. Between the divergence point and the smaller root of the heat capacity, solutions are thermally stable. Whereas, between the smaller root of heat capacity and the larger root of the temperature, solutions are thermally unstable. The larger root of heat capacity is located after the larger root of temperature. Although the heat capacity is positive after its larger root, since the temperature is negative here, no physical black hole exists in this region.

As for the AdS case, thermal stability depends on the number of divergences and the place of root. In the absence of divergence, solutions are thermally unstable between the root of temperature and the root of heat capacity. Whereas, after the root of heat capacity, solutions are physical and stable. In case of the existence of one divergence for heat capacity, interestingly, between the root of temperature and divergence of the heat capacity, and also between the divergence point of heat capacity and its root,

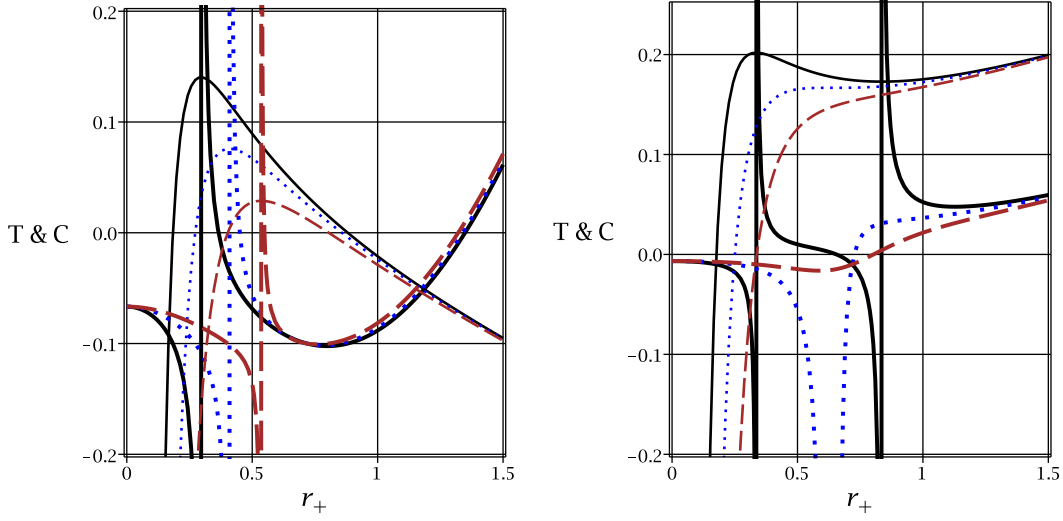


FIG. 2:  $C$  (bold lines) and  $T$  versus  $r_+$  for  $f(E) = g(\varepsilon) = 0.9$ ,  $k = \alpha = 1$ ,  $q(\varepsilon) = 0.2$  (continuous line),  $q(\varepsilon) = 0.2887$  (dotted line) and  $q(\varepsilon) = 0.4$  (dashed line). Left panel:  $\Lambda(\varepsilon) = 1$ ; Right panel:  $\Lambda(\varepsilon) = -1$ .

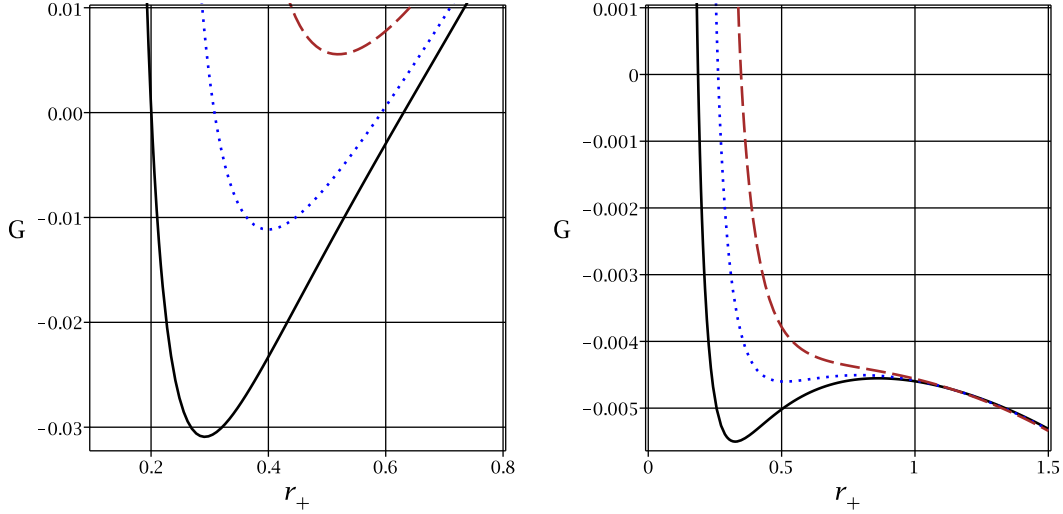


FIG. 3:  $G$  versus  $r_+$  for  $f(\varepsilon) = g(\varepsilon) = 0.9$ ,  $k = \alpha = 1$ ,  $q(\varepsilon) = 0.2$  (continuous line),  $q(\varepsilon) = 0.2887$  (dotted line) and  $q(\varepsilon) = 0.4$  (dashed line). Left panel:  $\Lambda(\varepsilon) = 1$ ; Right panel:  $\Lambda(\varepsilon) = -1$ .

the solutions are thermally unstable. The only stable region is after the root of heat capacity. This indicates that although there is phase transition for AdS black holes, the phase transition occurs between two unstable black holes. Thermally stable black holes are obtained only after the root of heat capacity. Finally, in case of two divergences, the only positive regions for heat capacity are between the smaller divergence of heat capacity and its root, and after larger divergence. Therefore, there are two phase transitions: one between smaller unstable and medium stable black holes; the other is between medium unstable and larger stable black holes. This is due to the fact that in the root of heat capacity which is located between the divergences, there is a change of signature taking place.

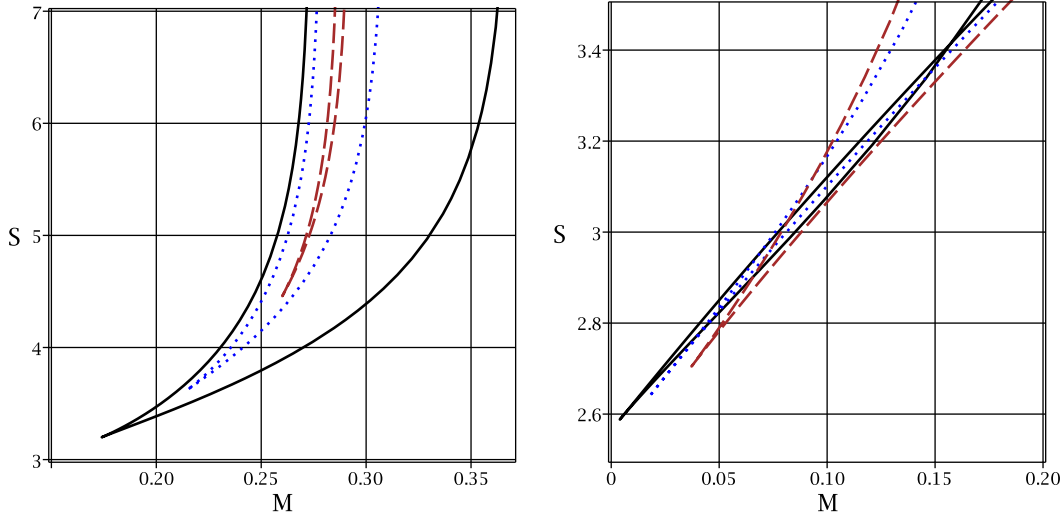


FIG. 4:  $S$  versus  $M$  for  $f(\varepsilon) = g(\varepsilon) = 0.9$ ,  $k = \alpha = 1$ ,  $q(\varepsilon) = 0.2$  (continuous line),  $q(\varepsilon) = 0.2887$  (dotted line) and  $q(\varepsilon) = 0.4$  (dashed line).  
Left panel:  $\Lambda(\varepsilon) = 1$ ; Right panel:  $\Lambda(\varepsilon) = -1$ .

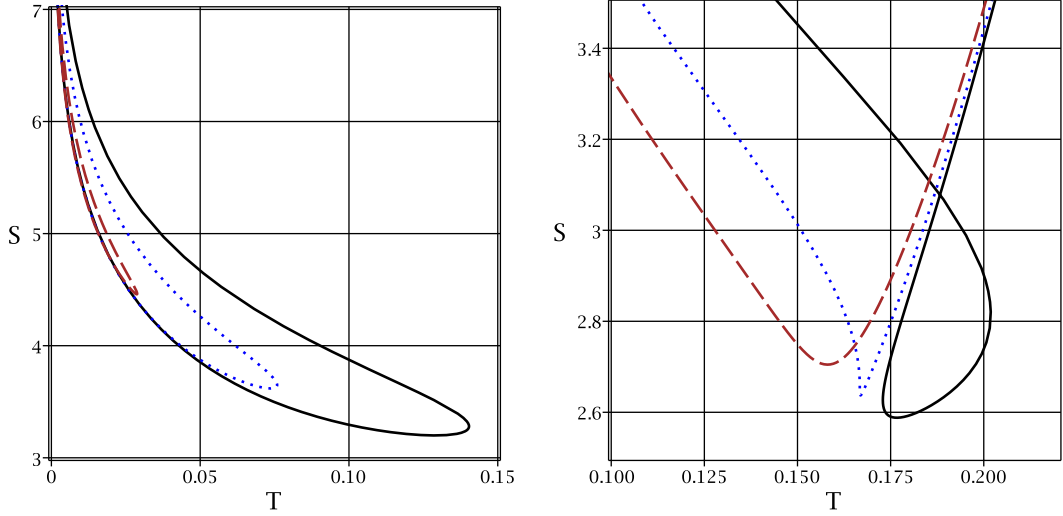


FIG. 5:  $S$  versus  $T$  for  $f(\varepsilon) = g(\varepsilon) = 0.9$ ,  $k = \alpha = 1$ ,  $q(\varepsilon) = 0.2$  (continuous line),  $q(\varepsilon) = 0.2887$  (dotted line) and  $q(\varepsilon) = 0.4$  (dashed line).  
Left panel:  $\Lambda(\varepsilon) = 1$ ; Right panel:  $\Lambda(\varepsilon) = -1$ .

One of the most interesting effects of the first-order correction could be detected through the high energy limit of heat capacity. It is a matter of calculation to show that high energy of this quantity is

$$\lim_{r_+ \rightarrow 0} C = -\frac{2}{3}\alpha - \frac{\pi q^2(\varepsilon) f^2(\varepsilon) + \frac{4}{3}\alpha k g^2(\varepsilon)}{6q^2(\varepsilon) g^2(\varepsilon) f^2(\varepsilon)} r_+^2 + \mathcal{O}(r_+^4).$$

Here, we see that high energy limit of the heat capacity is purely governed by correction parameter,  $\alpha$ , without any factor of other quantities. Considering the positive  $\alpha$ , one can find that the heat capacity is negative in the high energy limit. In addition, since the correction factor is not coupled with any

other quantity, it indicates that if the black hole vanishes, there is a non-zero heat capacity available which could mark the existence of the black hole. This means that all the information regarding the existence of the black hole is not lost and some of it remains in form of non-vanishing heat capacity. This is another important property of the first-order correction which shows the deviation from usual black holes thermodynamics. On the other hand, the asymptotical behavior of the heat capacity is given by

$$\begin{aligned} \lim_{r_+ \rightarrow \infty} C &= \frac{\pi r_+^2}{2g^2(\varepsilon)} - \frac{\pi k + 2\alpha\Lambda(\varepsilon)}{\Lambda(\varepsilon)} + \frac{2\pi q^2(\varepsilon) f^2(\varepsilon) \Lambda(\varepsilon) + kg^2(\varepsilon) (\pi k + 2\alpha\Lambda(\varepsilon))}{2\Lambda^2(\varepsilon) r_+^2} \\ &+ \mathcal{O}\left(\frac{1}{r_+^4}\right). \end{aligned} \quad (25)$$

Evidently, the asymptotical behavior of the solutions is governed only by gravitational part. This is due to fact that in the dominant term, no traces of the electric charge, the first-order correction, topological factor and cosmological constant are observable. Therefore, the asymptotical behavior is governed by gravitational part purely. It is worthwhile to mention that the effects of the first-order correction could be observed in the second and third dominant terms.

Next, we study the behavior of Gibbs free energy. According to the thermodynamical principle, the Gibbs free energy could be employed to extract the phase transition points. Phase transition points in Gibbs free energy can be present at extrema. Therefore, the existence of extrema in Gibbs free energy diagrams indicates that solutions enjoy thermal phase transitions in their structure. Unfortunately, due to the complexity of the obtained Gibbs free energy, it was not possible to obtain the extrema of it analytically. Therefore, we employed the numerical method (see Fig. 3). Evidently, for the dS case, Gibbs free energy enjoys the existence of a minimum in its structure. The place of this minimum is exactly the same as divergence of the heat capacity. Therefore, the phase transition point observed in the heat capacity coincides with the one in the Gibbs free energy. It is worthwhile to mention that Gibbs free energy, in this case, could enjoy one of the following cases as well: I) absence of root, II) the existence of one extreme root, and III) presences of two roots. The AdS case presents the larger variation in its behavior. It could have: I) only one root, II) one root with one extremum, and III) one root with two extrema. The extrema in any of the mentioned cases are located exactly where the heat capacity meets divergences.

As for the high energy limit, interestingly, similar to the heat capacity case, the high energy limit is governed by correction factor,  $\alpha$ ,

$$\begin{aligned} \lim_{r_+ \rightarrow 0} G &= -\frac{\alpha q^2(\varepsilon) g(\varepsilon) f(\varepsilon) \left[ 3 \ln\left(\frac{-q^2(\varepsilon) f(\varepsilon)}{8\sqrt{\pi} r_+^2}\right) - 2 \right]}{12\pi r_+^3} \\ &- \frac{4\alpha k g^2(\varepsilon) - \pi q^2(\varepsilon) f^2(\varepsilon) + 4\alpha k g^2(\varepsilon) \ln\left(\frac{-q^2(\varepsilon) f(\varepsilon)}{8\sqrt{\pi} r_+^2}\right)}{16\pi g(\varepsilon) f(\varepsilon) r_+} + \mathcal{O}(r_+), \end{aligned} \quad (26)$$

but contrary to heat capacity case, here, there is a coupling between correction term and electric charge part of the solutions. On the other hand, the dominant term in asymptotical behavior of the Gibbs free energy is the cosmological constant term without any coupling with correction term which can be seen from following:

$$\begin{aligned} \lim_{r_+ \rightarrow \infty} G &= \frac{\Lambda(\varepsilon) r_+^3}{48g^3(\varepsilon) f(\varepsilon)} - \frac{\left[ 8\alpha\Lambda(\varepsilon) \ln(r_+) + 4\alpha\Lambda(\varepsilon) \ln\left(\frac{-\Lambda(\varepsilon)}{8\sqrt{\pi} g^2(\varepsilon) f(\varepsilon)}\right) - (\pi k + 8\alpha\Lambda(\varepsilon)) \right] r_+}{16\pi g(\varepsilon) f(\varepsilon)} \\ &+ \frac{\frac{\alpha k g(\varepsilon)}{4\pi f(\varepsilon)} \left[ \ln\left(\frac{-\Lambda(\varepsilon)}{8\sqrt{\pi} g^2(\varepsilon) f(\varepsilon)}\right) + 1 + 2 \ln(r_+) \right] - \frac{q^2(\varepsilon) f(\varepsilon)}{16g(\varepsilon)}}{r_+} + \mathcal{O}\left(\frac{1}{r_+^3}\right). \end{aligned} \quad (27)$$

In general, one can state that the effects of the first-order correction term could be highly detected for small and medium black holes while for the large black holes, it is not on significant level.

Our next subject of the interest is phase diagrams for corrected entropy versus effective mass (Fig. 4) and temperature (Fig. 5).

For the case of entropy versus mass, evidently, irrespective of the background spacetime (being dS or AdS), there exists a minimum in which both the entropy and internal energy are minimum. The entropy for both of the cases of dS and AdS is an increasing function of the internal energy. In dS case, interestingly, two branches exist in which for every entropy, there exists at least two different internal energy. The only exception is the extremum point (minimum) in which the two branches coincided. As for the AdS case, the situation is same except for one of the diagrams. In this case, two points exist in which two branches coincide. One of them is the minimum that was discussed for the dS case, while the other one is after the minimum. Interestingly, at this point (see the continuous line in the right panel of Fig. 4), the place of branches is switched. Let's say that before this point, for any entropy, two internal energy exists: one belongs to branch *A* (right branch in Fig. 4) and the other one belongs to branch *B* (right branch in Fig. 4) in which internal energy of branch *B* is bigger than the one in branch *A*. After the mentioned point, the bigger internal energy will belong to branch *A* and the smaller one will be of branch *B*.

The situation in entropy versus temperature diagrams is different for dS and AdS cases. Here, for the dS case, the temperature has a maximum that can be acquired. The maximum is actually where entropy acquires its minimum. Here too, for every entropy, two temperature exist except for the minimum where both branches coincide. On the other hand, the AdS case situation is different. Here, there is no maximum present for the temperature while one can obtain a minimum for the entropy. Before the minimum, entropy is a decreasing function of the temperature, while after the minimum, the entropy will be an increasing function of the temperature. Interestingly, for specific cases (see the continuous line in the left panel of Fig. 5), it is possible for the two branches of entropy versus temperature to coincide in two points and form a closed cycle. In this case, the entropy is first a decreasing function of the temperature, then both of the temperature and entropy decreases to reach the minimum point. After that, the entropy becomes an increasing function of the temperature.

The plotted diagrams for the dS case have yet another property which was absent in AdS diagram except for the mentioned special case. This property is due to the fact that for every temperature there are two entropies while for every entropy, there are also two temperatures. In a manner, the plotted diagrams for the dS case are closed one. For the AdS diagrams, closed diagram was observed only for the special case where two coinciding points for the two branches exist. A simple comparison between these diagrams with those plotted before shows that this special case for AdS background is related to the presence of two divergences in the heat capacity diagrams. This confirms that entropy versus temperature diagrams recognize the existence of phase transition point in its structure. Here, we see that background spacetime has profound contributions to the thermodynamical structure of the black holes. Plotted diagrams for entropy versus temperature measures the changes in entropy by temperature fluctuation. Evidently, for the dS case, we come across a cyclic (closed) diagrams indicating the existence of bounds on values that temperature could acquire. On the other hand, for the AdS case, such closed cyclic diagrams were observed for specific values of different parameters but the existence of this cycle does not bound the temperature. In fact, it puts a bound on limits that entropy can acquire. Here, we see that the entropy could not vanish completely.

## V. CORRECTION VERSUS NON-CORRECTION

The final section of this paper is devoted to understand the effects of the first-order correction and compare it with the non-correction case. Here, we intend to see how the entropy and stability are modified due to contributions of the first-order correction. First of all, we have plotted diagrams for the entropy versus temperature in the absence of the first-order correction, i.e.  $\alpha = 0$ , in Fig. 6.

In the case of dS, interestingly, we observe that no cyclic like behavior is present and for vanishing the temperature, there are two positive values available for the entropy of the system. In this case, similar to the presence of correction, there is a maximum available for the temperature and a minimum for

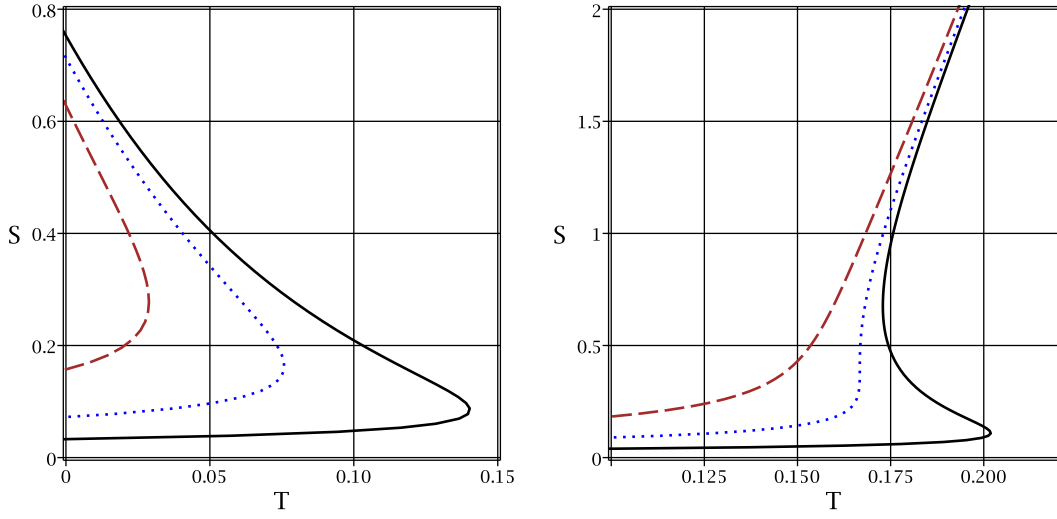


FIG. 6:  $S$  versus  $T$  for  $\alpha = 0$ ,  $f(\varepsilon) = g(\varepsilon) = 0.9$ ,  $k = 1$ ,  $q(\varepsilon) = 0.2$  (continuous line),  $q(\varepsilon) = 0.2887$  (dotted line) and  $q(\varepsilon) = 0.4$  (dashed line).  
Left panel:  $\Lambda(\varepsilon) = 1$ ; Right panel:  $\Lambda(\varepsilon) = -1$ .

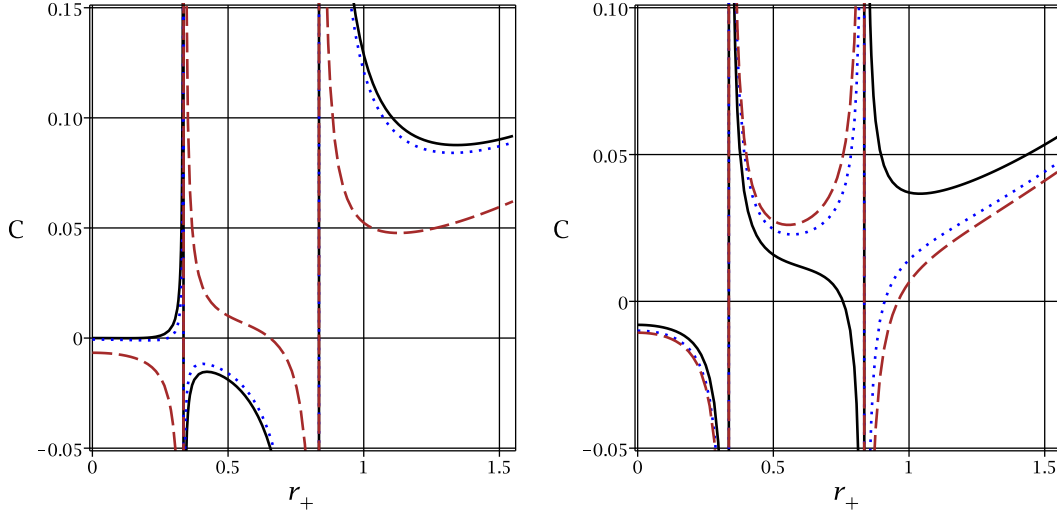


FIG. 7:  $C$  versus  $r_+$  for  $\Lambda(\varepsilon) = -1$ ,  $f(\varepsilon) = g(\varepsilon) = 0.9$ ,  $k = 1$  and  $q(\varepsilon) = 0.2$ .  
Left panel:  $\alpha = 0$  (continuous line),  $\alpha = 0.1$  (dotted line) and  $\alpha = 1$  (dashed line).  
Right panel:  $\alpha = 1.2$  (continuous line),  $\alpha = 1.5$  (dotted line) and  $\alpha = 1.6$  (dashed line).

entropy but contrary to correction case, the minimum of entropy and maximum of the temperature do not take place at the same point. In the correction case, for every entropy (temperatures), there exist two temperatures (entropies). In the absence of correction, for every temperature, there exist two entropies. The only exception is at the maximum of temperature.

The AdS case provides us with more interesting details. The dashed, dotted and continuous lines in the right panel of Fig. 6, respectively correspond to absence, one and two divergences in the heat capacity. In the absence of divergence, the entropy is an increasing function of the temperature. Interestingly, in case of divergence, there is only one extremum for the temperature and entropy. Except for this extremum,

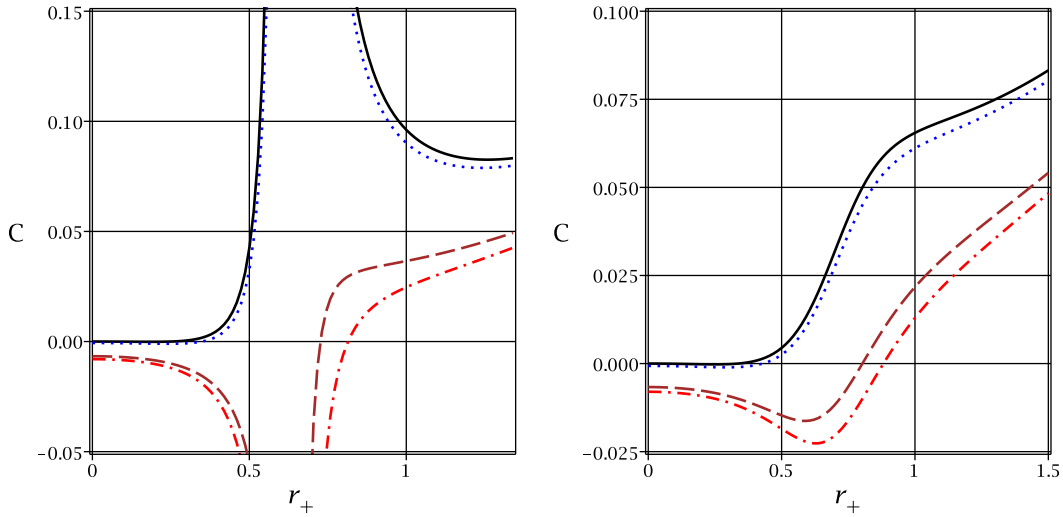


FIG. 8:  $C$  versus  $r_+$  for  $\Lambda(\varepsilon) = -1$ ,  $f(\varepsilon) = g(\varepsilon) = 0.9$ ,  $k = 1$ ,  $\alpha = 0$  (continuous line),  $\alpha = 0.1$  (dotted line),  $\alpha = 1$  (dashed line) and  $\alpha = 1$  (dashed-dotted line). Left panel:  $q(\varepsilon) = 0.2887$ ; Right panel:  $q(\varepsilon) = 0.4$ .

the entropy is an increasing function of the temperature. For the case of two divergences, we can divide the diagram into three regions. These regions are recognized by two temperatures,  $T_1$  and  $T_2$  which are essentially extrema. Before  $T_1$  ( $T < T_1$ ) and after  $T_2$  ( $T > T_2$ ), the entropy is an increasing function of the temperature and for every temperature, there exists only one entropy. For  $T = T_1, T_2$ , one can have two entropies, and interestingly, between these two temperatures ( $T_1 < T < T_2$ ), for any temperature, one can find three different entropies. For all of the plotted diagrams, in the absence of temperature, one can find a non-vanishing positive entropy. There are several significant differences between the corrected case and usual one for AdS spacetime: I) in the case of correction, a minimum was observed for the entropy in certain non-zero temperature, interestingly, for the non-corrected case, the minimum for entropy is obtained for the vanishing temperature, II) for the correction, in case of two divergency in the heat capacity, a cycle was observed for entropy versus temperature diagram, whereas, this cycle is not present in the usual non-corrected case, and III) in the correction case, for every entropy, there exists at least two temperatures except for two points: one is at the minimum of entropy and the other one, which is more interesting, is when two branches of  $A$  and  $B$  meet. This coincidence between the branches is due to the fact that there is a cycle in correction case for AdS spacetime. It is worthwhile to mention that for the correction case, one can point out three distinctive temperatures:  $T'_1$ ,  $T'_2$  and  $T_c$ , where  $c$  stand for coincidence. In case of  $T < T'_1$  and  $T > T'_2$ , for every temperature there exists one entropy. On the other hand, in case of  $T'_1 < T < T_c$  and  $T_c < T < T'_2$ , each temperature has three different entropies. Interestingly, in case of  $T = T'_1, T'_2, T_c$  each temperature is mapped with two different entropies. The three mentioned points highlight the significant differences in thermodynamical picture of the entropy measured by the fluctuation of temperature comparing to the usual case of without any correction. For further clarification, we compare the heat capacity of the two cases.

In the previous section, we point out that denominator of the heat capacity is not affected by the first-order correction. This indicates that phase transition points (divergences of the heat capacity) are independent of the first-order correction. On the contrary, the numerator of the heat capacity was highly correction dependent. The first result of this dependency is that temperature and heat capacity do not share the same root anymore (it is worthwhile to mention that one of the important properties of the non-correction case is the coincidence between the roots of temperature and heat capacity). The second important result is that thermal stability conditions are determined by the value of correction parameter. In order to highlight this, we have plotted the diagrams for the AdS case in Figs. 7 and 8.

In case of the two divergences in the heat capacity, the effects of correction could be categorized into three cases with two distinctive correction parameter,  $\alpha_1$  and  $\alpha_2$ . I) For  $\alpha < \alpha_1$ , the general behavior of the heat capacity is similar to the one in the non-correction case with slight modification in place of the root. II) For  $\alpha_1 < \alpha < \alpha_2$ , the behavior of heat capacity, hence stability conditions are modified on a significant level. Before the smaller divergence, no root is present and the heat capacity is negative. Between the divergences, a root is observed for the heat capacity. Before root, the heat capacity is positive while after it until the larger divergence, it is negative. After the larger divergence, the heat capacity is positive. Therefore, the stable regions are between smaller divergence and root, and after the larger divergence. III) for  $\alpha_2 < \alpha$ , the root of heat capacity is observed after larger divergence. Before the smaller divergence and, between larger divergence and root, the heat capacity is negative which indicates thermal instability in these regions. Between the divergences and after the root, the heat capacity is positive and solutions are thermally stable.

In case of one divergence, the effects of correction are divided into two groups. I) For small values of correction parameter, the root of heat capacity is slightly modified to larger values of horizon radius and the stability conditions are same as those derived for the non-correction case. II) for sufficiently large correction parameter, the place of root is changed. It will be after the divergence. Before divergence and, between divergence and root, the heat capacity is negative and solutions are thermally unstable. The only thermal stable state exists after the root. For the case in which the heat capacity does not have any divergence, the only effect of the first-order correction is changing the place of root. In this case, root is an increasing function of this parameter.

To summarize, we observed that the entropy, as a function of the temperature, for the correction case has a significant deviation from the non-correction case. Thermodynamically speaking, the existence of correction introduces specific properties into system, for example, these are cyclic/closed diagrams and existence of a minimum for entropy for non-zero temperature. The stability conditions were proved to be highly sensitive to the variation of the correction parameter. While for small values of it, the stability condition was not modified, for sufficiently large values, the thermodynamical stability, hence thermodynamical structure was modified on a significant level. This signals us with the fact that deviation from the non-correction case with the corrected one depends on values that correction parameter could acquire.

## VI. CONCLUSIONS

In this paper, we have investigated the effects of the first-order correction on thermodynamical behavior of the 4-dimensional charge black holes in the presence of gravity's rainbow. Through our study, we have confirmed that modification in entropy (the first-order logarithmic correction) resulted into modifications in mass (internal energy), heat capacity and free energy, whereas, interestingly, no effects were observed for temperature. This indicated that the effects of consideration of the first-order correction on entropy and internal energy are on a level which leaves the temperature unaffected. This situation is very similar to isothermal process in which internal energy and entropy is changed while the temperature remains fixed.

One of the significant effects of the correction has been found in the contexts of heat capacity, more precisely, in the context of thermal stability of the solutions. Surprisingly, the phase transition points (divergences of the heat capacity) were not affected by the presence of the first-order correction while the number of roots, therefore, the signature of heat capacity was highly modified to a level of introducing new thermal stability conditions and presence of multiple stable/unstable phases. Remarkably, even in case of AdS black holes, the phase transition between two unstable black holes was observed. This is a significant difference observed in the case where the first-order correction is absent.

Generally speaking, the highest contribution of the first-order correction was on high energy limit of different quantities. Especially, it was shown that high energy limit of heat capacity is purely governed by the correction parameter. Moreover, in evaporation of the black holes, a trace of its existence could be detected through the remnant of heat capacity in form of correction parameter. Furthermore, the effects



of the first-order correction could significantly be observed for medium black holes as well. However, for large black holes, the contributions of this correction was either absent or not present on a significant level.

The study of the entropy versus temperature revealed several interesting facts. First of all, it was shown that dS and AdS cases have a completely different thermodynamical picture and limitations. For example, the measurement of entropy as a function of fluctuation of temperature showed that dS case puts an upper bound on values that temperature that can be acquired and a cyclic behavior wasn't observed. On the contrary, for the AdS case, a lower bound was observed for the entropy, while the cyclic behavior could be detected for special cases and there were no upper bound on the temperature. Furthermore, it was observed that for the cases of two divergences in the heat capacity for AdS case, the entropy diagrams also recognizes the existence of such discontinuity in their structure.

The study conducted in this paper confirmed that deviation from thermodynamical properties of the non-correction case with the first-order corrected entropy is determined by the correction parameter,  $\alpha$ . Especially, it was shown that for the cases of existence of divergence in the heat capacity, hence phase transition points, the thermodynamical stability was highly dependent on the value of correction parameter. This indicates that thermodynamical structure of the black holes in the presence of the first-order correction is determined by the value of correction parameter and the corrected case enjoys larger classes of possibility for its thermodynamical structure.

In fact, we are faced with a very important question: are all the classes provided with the first-order correction physically acceptable? If the answer to this question is positive this means that correction parameter is not bounded and it can acquire any value. But then again, we are using the term *correction* in our analogy. This term implies that we are expecting to see modifications on a specific level. Therefore, we have to label some of the possibilities provided by the first-order correction as *non-physical ones*. This requires finding an upper/lower limit on values that correction parameter could acquire. To address this issue, there are following two approaches that one can employ. I) By considering that the entropy correction has holographical origins, it is possible to find the bound on values of the correction parameter by studying superconductivity properties or diamagnetic/paramagnetic phase transitions and phases. This enables us to rule out the non-physical cases and puts bounds on the values of correction parameter. II) The second method is to use the properties of extended phase space. Recently, it was shown that by this consideration, one can find compressibility coefficient and define the speed of sound for black holes. Using the fact that the speed of sound could not exceed the speed of light, one is able to recognize the physically allowed possibilities provided by the first-order correction and put a limit on correction parameter. The only shortcoming of this approach is the fact that this method is limited to the cases of negative cosmological constant. This is due to fact that extended phase space is constructed by replacing the negative cosmological constant with thermodynamical pressure. We leave these issues for future works.

**Acknowledgements:** S. H. Hendi and B. Eslam Panah thank Shiraz University Research Council. The work of S. H. Hendi has been supported financially by the Research Institute for Astronomy and Astrophysics of Maragha, Iran.

- 
- [1] P. Horava, Phys. Rev. D **79**, 084008 (2009).
  - [2] P. Horava, Phys. Rev. Lett. **102**, 161301 (2009).
  - [3] R. Gregory, S. L. Parameswaran, G. Tasinato and I. Zavala, JHEP **12**, 047 (2010).
  - [4] P. Burda, R. Gregory and S. Ross, JHEP **11**, 073 (2014).
  - [5] K. Goldstein, N. Iizuka, S. Kachru, S. Prakash, S. P. Trivedi and A. Westphal, JHEP **10**, 027 (2010).
  - [6] G. Bertoldi, B. A. Burrington and A. W. Peet, Phys. Rev. D **82**, 106013 (2010).
  - [7] M. Kord Zangeneh, A. Sheykhi and M. H. Dehghani, Phys. Rev. D **92**, 024050 (2015).
  - [8] J. Tarrío and S. Vandoren, JHEP **09**, 017 (2011).
  - [9] S. S. Gubser and A. Nellore, Phys. Rev. D **80**, 105007 (2009).
  - [10] Y. C. Ong and P. Chen, Phys. Rev. D **84**, 104044 (2011).

- [11] M. Alishahiha and H. Yavartanoo, *Class. Quantum Gravit.* **31**, 095008 (2014).
- [12] S. Kachru, N. Kundu, A. Saha, R. Samanta and S. P. Trivedi, *JHEP* **03**, 074 (2014).
- [13] J. Magueijo and L. Smolin, *Phys. Rev. Lett.* **88**, 190403 (2002)
- [14] J. Magueijo and L. Smolin, *Class. Quantum Gravit.* **21**, 1725 (2004).
- [15] A. F. Ali and M. M. Khalil, *Europhys. Lett.* **110**, 20009 (2015).
- [16] J. J. Peng and S. Q. Wu, *Gen. Relativ. Gravit.* **40**, 2619 (2008).
- [17] R. Garattini and E. N. Saridakis, *Eur. Phys. J. C* **75**, 343 (2015).
- [18] A. F. Ali, *Phys. Rev. D* **89**, 104040 (2014).
- [19] P. Galan and G. A. Mena Marugan, *Phys. Rev. D* **74**, 044035 (2006).
- [20] Y. Ling, X. Li and H. Zhang, *Mod. Phys. Lett. A* **22**, 2749 (2007).
- [21] J. -J. Peng and S. -Q. Wu, *Gen. Rel. Grav.* **40**, 2619 (2008).
- [22] H. Li, Y. Ling and X. Han, *Class. Quant. Grav.* **26**, 065004 (2009).
- [23] Y. Gim and W. Kim, *JCAP* **10**, 003 (2014).
- [24] S. H. Hendi, S. Panahiyan, B. Eslam Panah, M. Momennia, *Eur. Phys. J. C* **76**, 150 (2016).
- [25] Y. -W. Kim, S. K. Kim and Y. -J. Park, *Eur. Phys. J. C* **76**, 557 (2016).
- [26] Z. -W. Feng, S. -Z. Yang, H. -L. Li and X. -T. Zu, [arXiv:1608.06824].
- [27] Z. -W. Feng and S.-Z. Yang, *Phys. Lett. B* **772**, 737 (2017).
- [28] S. H. Hendi, S. Panahiyan, B. Eslam Panah, M. Faizal and M. Momennia, *Phys. Rev. D* **94**, 024028 (2016).
- [29] S. Alsaleh, *Eur. Phys. J. Plus* **132**, 181 (2017).
- [30] S. H. Hendi, B. Eslam Panah and S. Panahiyan, *Phys. Lett. B* **769**, 191 (2017).
- [31] S. H. Hendi, S. Panahiyan, S. Upadhyay and B. Eslam Panah, *Phys. Rev. D* **95**, 084036 (2017).
- [32] R. Garattini, *JCAP* **06**, 017 (2013).
- [33] S. H. Hendi, B. Eslam Panah, S. Panahiyan, M. Momennia, *Adv. High Energy Phys.* **2016**, 9813582 (2016).
- [34] S. H. Hendi, M. Faizal, B. Eslam Panah and S. Panahiyan, *Eur. Phys. J. C* **76**, 296 (2016).
- [35] S. H. Hendi, B. Eslam Panah, S. Panahiyan and M. Momennia, *Eur. Phys. J. C* **77**, 647 (2017).
- [36] R. Garattini and B. Majumder, *Nucl. Phys. B* **883**, 598 (2014).
- [37] R. Garattini and F. S. N. Lobo, *Eur. Phys. J. C* **74**, 2884 (2014).
- [38] S. H. Hendi, G. H. Bordbar, B. Eslam Panah and S. Panahiyan, *JCAP* **09**, 013 (2016).
- [39] R. Garattini and G. Mandanici, *Eur. Phys. J. C* **77**, 57 (2017).
- [40] B. Eslam Panah, et al., *Astrophys. J.* **848**, 24 (2017).
- [41] R. Garattini and F. S. N. Lobo, [arXiv:1512.04470].
- [42] D. Momeni, S. Upadhyay, Y. Myrzakulov and R. Myrzakulov, *Astrophys Space Sci.* **362**, 148 (2017).
- [43] A. F. Ali, M. Faizal and M. M. Khalil, *JHEP* **12**, 159 (2014).
- [44] I. P. Lobo, N. Loret and F. Nettel, *Eur. Phys. J. C* **77**, 451 (2017).
- [45] C. Leiva, J. Saavedra and J. Villanueva, *Mod. Phys. Lett. A* **24**, 1443 (2009).
- [46] A. Awad, A. F. Ali and B. Majumder, *JCAP* **10**, 052 (2013).
- [47] S. H. Hendi, M. Momennia, B. Eslam Panah and M. Faizal, *Astrophys. J.* **827**, 153 (2016).
- [48] Y. Ling, *JCAP* **08**, 017 (2007).
- [49] S. H. Hendi, M. Momennia, B. Eslam Panah and S. Panahiyan, *Phys. Dark Universe* **16**, 26 (2017).
- [50] Y. Ling and Q. Wu, *Phys. Lett. B* **687**, 103 (2010).
- [51] G. Amelino-Camelia, M. Arzano, G. Gubitosi and J. Magueijo, *Phys. Rev. D* **88**, 041303, (2013).
- [52] G. Santos, G. Gubitosi, G. Amelino-Camelia, *JCAP* **08**, 005 (2015).
- [53] J. Tao, P. Wang and H. Yang, *Phys. Rev. D* **94**, 064068 (2016).
- [54] M. Khodadi, K. Nozari and H. R. Sepangi, *Gen. Rel. Grav.* **48**, 166 (2016).
- [55] S. H. Hendi, *Gen. Relativ. Gravit.* **48**, 50 (2016).
- [56] S. Gangopadhyay and A. Dutta, *Euro. Phys. Lett.* **115**, 50005 (2016).
- [57] P. Rudra, M. Faizal, A. F. Ali, *Nucl. Phys. B* **909**, 725 (2016).
- [58] H. Itoyama, A. Mironov and A. Morozov, *Phys. Lett. B* **771**, 180 (2017).
- [59] F. Brighenti, G. Gubitosi and J. Magueijo, *Phys. Rev. D* **95**, 063534 (2017).
- [60] M. Assanioussi and A. Dapor, *Phys. Rev. D* **95**, 063513 (2017).
- [61] M. A. Gorji, K. Nozari and B. Vakili, *Phys. Lett. B* **765**, 113 (2017).
- [62] D.V. Fursaev, *Phys. Rev. D* **51**, R5352 (1995).
- [63] R. B. Mann and S.N. Solodukhin, *Nucl. Phys. B* **523**, 293 (1998).
- [64] R. K. Kaul and P. Majumdar, *Phys. Rev. Lett.* **84**, 5255 (2000).
- [65] S. Kloster, J. Brannlund and A. DeBenedicts, *Class. Quantum Grav.* **25**, 065008 (2008).
- [66] S. Das, P. Majumdar and R. K. Bhaduri, *Class. Quant. Grav.* **19**, 2355 (2002).
- [67] S. Carlip, *Class. Quantum Grav.* **17**, 4175 (2000).
- [68] S. Upadhyay, S. Soroushfar and R. Saffari, [arXiv:1801.09574].
- [69] S. Upadhyay and B. Pourhassan, [ arXiv:1711.04254].

- [70] S. Upadhyay, Phys. Lett. B **775**, 130 (2017).
- [71] B. Pourhassan, S. Upadhyay, H. Saadat and H. Farahani, Nucl. Phys. B **928**, 415 (2018).
- [72] B. Pourhassan, S. Upadhyay and H. Farahani, [arXiv:1701.08650].
- [73] S. Upadhyay, B. Pourhassan and H. Farahani, Phys. Rev. D **95**, 106014 (2017).
- [74] B. Pourhassan, M. Faizal and U. Debnath, Eur. Phys. J. C **76**, 145 (2016).
- [75] J. Sadeghi and B. Pourhassan, JHEP **12**, 026 (2008).
- [76] J. Sadeghi, M. R. Setare, B. Pourhassan, and S. Heshmatian, Eur. Phys. J. C **61**, 527 (2009).
- [77] J. Sadeghi, B. Pourhassan, and F. Rahimi, Can. J. Phys. **92**, 1638 (2014).